Transient induced effects on electrostatic and magnetic fluctuations in the SOL of W7-X

M. Spolaore[1,2], C. Killer[3], R. Cavazzana[1], P. Agostinetti[1,2], D. Cipciar[3], R. Ghiraldelli[2], K. Rahbarnia[3], N. Vianello[1,2] and the W7-X Team

[1]*Consorzio RFX (CNR, ENEA, INFN, Università di Padova, Acciaierie Venete SpA), Padova, Italy*

[2]*Istituto per la Scienza e Tecnologia dei Plasmi, ISTP-CNR, Padova, Italy*

[3]*Max Planck Institut für Plasmaphysik, Greifswald, Germany*

Electromagnetic filamentary turbulent structures are found to characterize the edge region of different magnetic configurations including Reversed Field Pinch, stellarator and tokamak [1, 2, 3, 4, [5]], where strong currents are associated also to ELM filamentary structures [6,7]. The study of those phenomena in W7-X stellarator [8] is of particular interest as the electromagnetic features of filaments are expected to become more relevant with the increase of the local plasma beta [5]. For the study of electrostatic and magnetic fluctuations characterizing the edge region of the stellarator experiment W7-X, a specifically designed insertable probe head was constructed within the framework of EUROfusion in collaboration between Consorzio RFX, IPP Greifswald and FZJ Julich. The probe head, named High Resolution Probe (HRP) [9,10], was conceived to be installed on the mid-plane multi-purpose fast reciprocating manipulator [11] on W7-X. It is equipped [10] with two triple probes and four Mach probes located at different radial position, and three tri-axial coils arranged on a cross-field plane, so that the fluctuations of radial, poloidal and toroidal components of magnetic fluctuations (b_{rad}, b_{pol}, b_{tor}) are available and as well the direct measurement of current density fluctuations, $J_{par} = (\nabla \times b)_{par}/\mu_0$, parallel to the main magnetic field B_0.

The probe was installed on MPM manipulator and collected measurements in a variety of magnetic configurations and scenarios. The possibility, granted by the MPM system, of regulating the duration of inserted position was exploited, allowing the plasma monitoring in a stationary position up to 0,6 s for each insertion plunge. In its upgraded , RFX-HRP1,version the diagnostics, accounting also for an optimized orientation [12] of the probe head tailored for the Standard and High-Mirror magnetic configurations, was used during the OP2.3 experimental campaign. In fig. 1 an example of time evolution of the (b_{rad}, b_{pol}, b_{tor}) components of the most inserted coil are shown during a single plunge insertion. It results that $b_{tor} << b_{rad}$, b_{pol}, confirming the good orientation of the diagnostics with respect to the main magnetic field.

The multiple, long-lasting, insertions scheme opens the possibility to monitor transient conditions in the plasma edge, such as improved plasma performance or density ramp or steps. In particular strong indications of a change in features of magnetic fluctuations in the edge region is observed accompanying the diamagnetic energy (W_{dia}) transients, obtained with different scenarios.

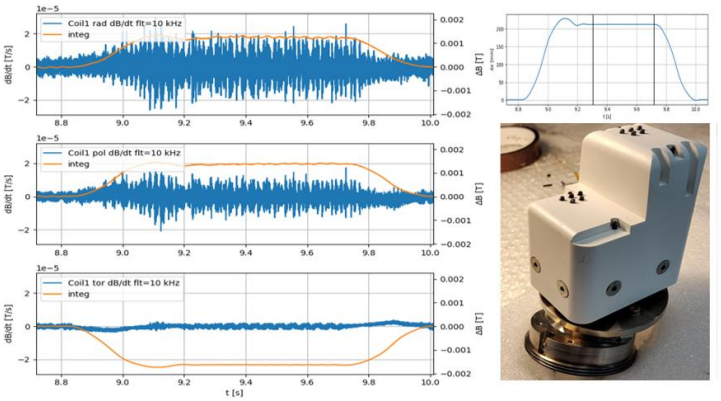

Figure 1: Example of timeseries of the 3 different components of magnetic field fluctuations measured by the 3-axial probe on the deepest position in the RFX-HRP1 probe. Coil data calibrated according to the winding area (left). Probe head picture and position excursion during a single plunge (right).

As an example, in fig.2 is shown a case of high-performance scenario at B_0 = - 2.62 T, where, combining NBI and pellet injection, W_{dia} reached values up to 17 10^2 kJ, the general shot parameters are reported in fig.2 (left).

The multiple MPM plunges, allowed the monitoring of the time evolution of edge parameters with the RFX-HRP1 probe accompanying the W_{dia} different phases. In fig.2(right) the behaviour of the all magnetic sensors installed on the probe are shown. In particular the third plunge with stationary phase starting at t= 4 s, catches the abrupt increase of the W_{dia} up to the maximum value and a corresponding strong increase of the magnetic fluctuation levels is clearly

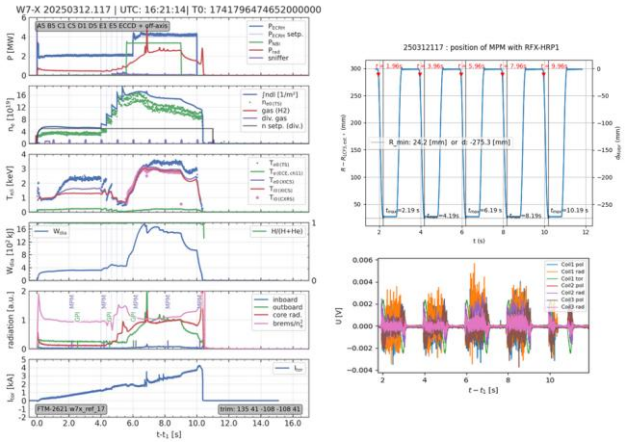

Figure 2: General plasma parameters for a discharge with strong Wdia transient (left); Time excursion of the probe insertions and corresponding raw data of collected by all magnetic coils (db/dt) into the probe head.

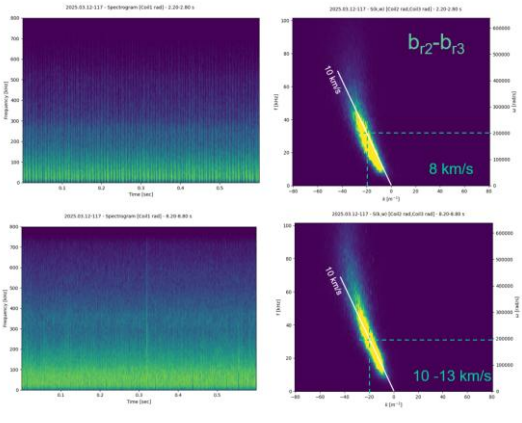

Figure 3: Spectrograms of br1 fluctuations (left); S(k, ω) cross-spectral analysis for br2 and br3 magnetic fluctuations. Data from magnetic coils collected during plunge 1 and plunge 3.

visible. A more detailed investigation is shown in fig. 3, where the spectrograms of the b_{rad1}, the most inserted coil, is evaluated comparing the plunge 1 and plunge 3 respectively.

The analysis evidences a spreader frequency range in the plunge 3, involving a high frequency range from 300 kHz to 700 kHz, not visible in the lower W_{dia} phase, analogous behaviour was observed by Mirnov coils system [13].

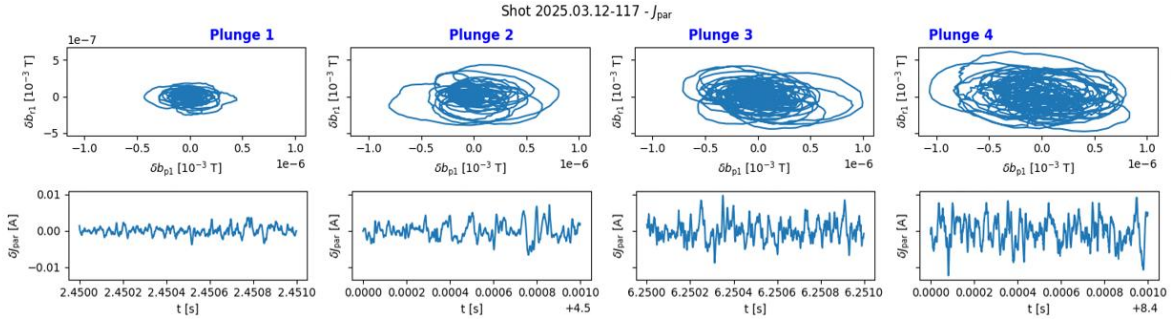

Figure 3: Comparison of the four plunges in the shot. Phase-space plot for the b_{r1} and b_{p1} magnetic fluctuations (top) and current density fluctuations (bottom).

A further information is provided by the velocity propagation of magnetic fluctuations along the poloidal direction, as obtained by the S(k, ω), cross-spectral analysis, with wavenumber k and angular frequency ω, of the two coils (b_{rad2}, b_{rad3}) located at the same radial position, but poloidally spaced by 39 mm. A clear dominant velocity propagation is visible starting from about 8 km/s in the low W_{dia} phase increasing of about 25% in the highest performance phase, where also an even higher velocity component characterizing the range > 50 kHz. The evaluation of the current density fluctuations in the component parallel to the main magnetic field is provided in fig. 3. The picture refers to a time series sample of 1 ms selected as representative within each plunge series. From left to right the W_{dia} increases and a clear increase of J_{par} fluctuation intensity accompanies this transient. To gain insight on the features of δJ_{par} the phase-space plot in the corresponding selected time series for each plunge are shown

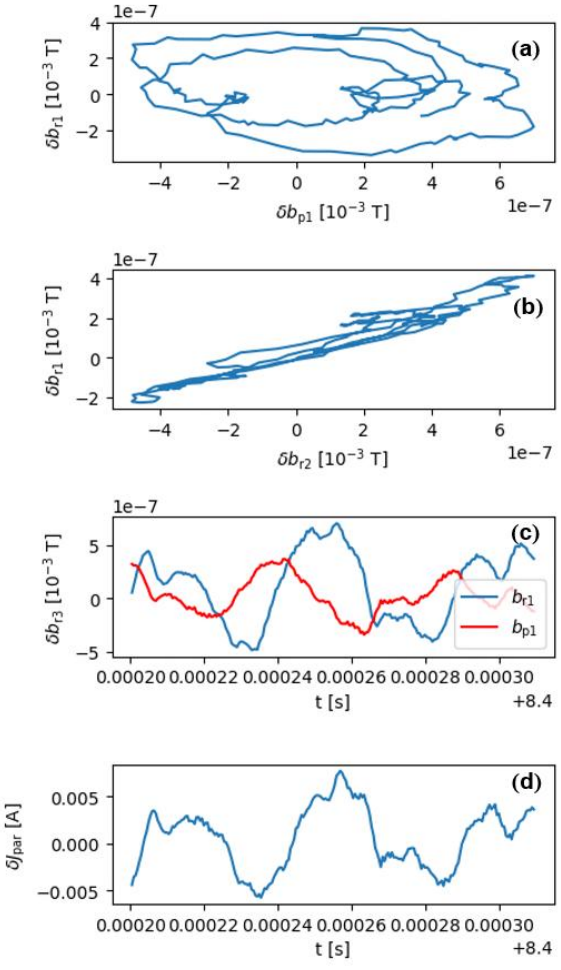

Figure 4: Details of a single current density peak measures during plunge 4.

in the top part of figure. The latter analysis was performed accounting the cross-field components of the most inserted coil: it turns out that besides the already mentioned increase of the magnetic fluctuation level with W_{dia} growing, the cross-field magnetic components are arranged in a circular shape, with average increasing size as moving from plunge 1 to plunge 4. This feature indicates a phase shift of $\pi/2$ between δb_{r1} and δb_{p1} that represents signature of current density fluctuation as filaments, oriented along the main magnetic field direction. To better study this feature, a close-up view around a single current density peak occurring during the last plunge is shown in fig. 4. It emerges that a the δJ_{par} is associated to circular shaped phase-space plot (fig4a) with evidence of $\pi/2$ shifted cross-field components, as confirmed also in the third panel of fig. 4c. As for comparison the phase-space plot of δb_{r1} and δb_{r2} a completely different behavior (fig. 4b), indicating a substantial coherence among the two coils radially spaced by 33 mm.

The combination of tri-axial magnetic coil allows to identify the signature of *current density fluctuations*, with signature of filaments, more evident and intense as the W_{dia} increases. Analogous results were obtained in the investigation of density ramp (up to $n_e \sim 2\ 10^{20}\ m^{-3}$).

The two cases are analogous except the behavior of velocity propagation of magnetic fluctuations: decreasing with density ramp, but increasing for the highest W_{dia} monitored.

In conclusion the RFX-HRP1 probe allowed to monitor in detail the edge region of W7-X experiment, during high performance scenarios. As a next step in the study, the effects related to the local magnetic topology in the region of measurements are to be evaluated in the different magnetic configuration explored.

This work has been carried out within the framework of the EUROfusion Consortium, funded by the European Union via the Euratom Research and Training Programme (Grant Agreement No 101052200 — EUROfusion). Views and opinions expressed are however those of the author(s) only and do not necessarily reflect those of the European Union or the European Commission. Neither the European Union nor the European Commission can be held responsible for them.

References

[1] M. Spolaore et al, Phys. Rev. Lett. 102, 165001 (2009)
[2] N. Vianello et al. Nucl. Fusion 50, 042002 (2010).
[3] I. Furno et al., Phys. Rev. Lett. 106, 245001 (2011).
[4] Grenfell, G., et al. Nuclear Fusion 60.12 (2020): 126006.
[5] Spolaore, M., et al. Physics of Plasmas 22.1 (2015)
[6] N. Vianello et al Phys. Rev. Lett. 106, 125002 (2011)
[7] M. Spolaore et al. Nuclear Materials and Energy 12 (2017) 844–851; M. Spolaore IAEA 2021 EX/P5-24
[8] O. Grulke et al 2026 Nucl. Fusion 66 116003
[9] P. Agostinetti et al. IEEE Transactions on Plasma Science 46.5 (2018): 1306.
[10] M. Spolaore, et al. Journal of Instrumentation 14.09 (2019): C09035.
[11] D. Nicolai, et al., Fusion Eng. Des. 123 (2017) 960-964
[12] C. Killer et al., Journal of Instrumentation 17.03 (2022): P03018.
[13] K Rahbarnia et al 2021 Plasma Phys. Control. Fusion 63 015005